Stanford Exploration Project, Report 125, January 16, 2007, pages 75–89

Stanford Exploration Project, Report 125, January 16, 2007, pages 75–89

/footerSEP–125

Image-space surface-related multiple prediction

Brad Artman and Ken Matson

ABSTRACT

The first step in surface-related multiple elimination (SRME) is prediction of the multiples from the recorded seismic data. Adaptive or pattern-based subtraction techniques are often then employed to eliminate the multiples from the data to isolate primary reflections. The malleable framework of shot-profile depth migration can be easily modified to produce the migration of the conventional surface-related multiple prediction (SRMP) during the course of a shot-profile migration with the (small) additional cost of an extra imaging condition. There may be several advantages to removing the multiples in the image space as the kinematics of events are simpler and the image-space volume is smaller than the data space for subtraction.

Image-space multiple prediction (IS-SRMP) takes advantage of the commutability of convolution and extrapolation. Casting the multiple prediction problem in terms of a migration imaging condition immediately suggests a deconvolutional variant. A deconvolutional implementation (dividing the multiple model by a power spectrum) increases the bandwidth of the IS-SRMP result to a similar range as the conventional image which aids in subtraction.

INTRODUCTION

It is well known that removing multiples from seismic data is an imperative to producing interpretable images of the subsurface. Multiple attenuation has a rich history in the geophysical literature ranging from methods that try to predict and remove the multiples from the seismic data to methods that use a differential characteristic between primaries and multiples as a discriminator and the basis for separating the two types of events (Weglein, 1999).

Prediction of the kinematics of multiple reflections by convolution of recorded data was first suggested by Anstey and Newman (1966). Due to amplitude and bandwidth inconsistencies associated with convolution, direct subtraction of multiples thus predicted was not possible. Tsai (1985) suggests modeling the waveform of the multiples to subtract events at times calculated by convolution from the data. The surface-related multiple elimination (SRME) method (Verschuur et al., 1992; Berkhout and Verschuur, 1997) convolves traces within shot-gathers to predict multiples (surface-related multiple prediction, SRMP) followed by an iterative subtraction scheme to eliminate them from the data. Alternatively, after predicting multiples, via convolution or filter-based methods, Guitton (2005) uses a pattern-based subtraction technique that resembles the match filter application described in Biersteker (2001).

While the above references all operate in the data domain, authors have also suggested removing multiples in the image space, after migration (Sava and Guitton, 2003, 2005; Alvarez et al., 2004). There are several motivators for attacking multiples in the image space. First, the image space is usually much smaller than the data space. Second, given a reasonably accurate velocity model, the kinematics of the image domain are simplified. Appropriately migrated primary events have little to no residual moveout, and multiples, migrated with velocities that are too fast, have predictable concave-down residual moveout in angle-domain common-image gathers. Alternatively, one could migrate the data and a multiple prediction separately and subtract the two image volumes. This is probably a prohibitively expensive strategy without obvious merit. However, because null-traces are filled during extrapolation steps through wave-front healing, multiple predictions in the image space may be more continuous and accurate in 3D.

We extend the SRMP approach to the image domain through the commutability of wavefield extrapolation and convolution to produce a multiple prediction in the image domain without needing to migrate two data volumes. Our approach is directly analogous to SRMP, though the prediction is calculated during the course of a shot-profile migration. The multiple prediction produced in the image space with this technique is exactly that which would be computed by migrating the multiple prediction produced by SRMP convolutions. The predicted multiples are then removed from the data via adaptive subtraction or pattern-matching techniques. The added cost of IS-SRMP is only a second imaging condition and writing out a second file the size of the migrated image. Because extrapolation dominates the cost of the shot-profile migration scheme, IS-SRMP does not significantly increase the migration cost.

We will develop the image-space surface related multiple prediction (IS-SRMP) technique by combining the SRMP approach with a wave-equation shot-profile depth migration algorithm. The Sigsbee2B synthetic dataset, which represents the multiple problem associated with deepwater seismic imaging in the presence of complex salt bodies, is used to show the efficacy of the approach. Images as a function of reflection angle and deconvolutional variants of the imaging-conditions are presented and we discuss their respective benefits.

IMAGE-SPACE SRMP

To predict multiples in the image space, the transform from the data space (shot gathers) to the image space plays an integral role. The image space is the output of migration, which in this implementation, is produced with a shot-profile depth migration algorithm. Shot-profile wave-equation depth migration (Claerbout, 1971) is the cascade of two component operations: extrapolation, and imaging. The extrapolation is carried out with an anticausal wave-equation operator on the up-going wavefield, U, and a causal operator for the down-going wavefield, D. U is a shot record with traces placed along a wavefield axis $\mathbf{x}$. D is a zero valued wavefield, also defined along the axis $\mathbf{x}$ where a source function is placed at the location of the shot being migrated, $\mathbf{x}_s$. The wavefields are recursively extrapolated to all depths z using the one-way

Fourier domain solution to the wave-equation

$$U_{z+1}(\mathbf{k}_x;\mathbf{x}_s,\omega) = U_z(\mathbf{k}_x;\mathbf{x}_s,\omega)\exp(+i\omega k_z) \tag{1}$$

and

$$D_{z+1}(\mathbf{k}_x;\mathbf{x}_s,\omega) = D_z(\mathbf{k}_x;\mathbf{x}_s,\omega)\exp(-i\omega k_z)\,. \tag{2}$$

In this work, the form of the dispersion relation used to calculate the vertical wavenumber, k_z, is the phase-shift plus interpolation (PSPI) algorithm (Gazdag and Sguazzero, 1984), though the degree of complexity of the operator does not change the discussion herein. The importance of these equations is that the operator that extrapolates a wavefield from one depth level to the next is a diagonal square matrix.

The correlation based multi-offset imaging condition for shot-profile migration at each depth level z is (Rickett and Sava, 2002)

$$i_z(\mathbf{x},\mathbf{h}) = \sum_{\mathbf{x}_s}\sum_{\omega} U_z(\mathbf{x}+\mathbf{h};\mathbf{x}_s,\omega)D_z^*(\mathbf{x}-\mathbf{h};\mathbf{x}_s,\omega) \tag{3}$$

where the $*$ represents conjugation. Extraction of the zero lag of the correlations, by summation over ω, combines the energy in the two wavefields that is colocated at each depth level. Overlapping acquisition patches from the individual shots are stacked by the sum over $\mathbf{x}_s$.

SRME is also a two component process: Multiple prediction and subtraction. Acknowledging the approximation of autoconvolving raw data traces rather than convolving data with only primaries, the prediction step (SRMP) can be written in the Fourier domain (Berkhout and Verschuur, equation 13f, 1997)

$$M(\mathbf{x}_g;\mathbf{x}_s,\omega) = \sum_{\mathbf{x}_a} R(\mathbf{x}_g;\mathbf{x}_a,\omega)R(\mathbf{x}_a;\mathbf{x}_s,\omega)\,, \tag{4}$$

where R is the data-space volume of shot-gathers defined at geophone and source locations on the acquisition surface. Equation 4 is a trace-by-trace operation to produce the multiple prediction with any geophone-source, $(\mathbf{x}_g,\mathbf{x}_s)$, combination by convolving each trace of every shot gather with all the others followed by summing over the convolution index $\mathbf{x}_a$. Note however, the similarity of the SRMP equation to the imaging condition of shot-profile migration, equation 3.

Wave-equation extrapolation is performed on wavefields where data and source-functions are used as initial conditions to propagate energy into the subsurface. To begin, traces at locations $\mathbf{x}_g$ are inserted into a zero-valued wavefield defined along the axis $\mathbf{x}$ as depicted in Figure 1. Although data-space SRMP is a trace-by-trace operation, equation 4 can be redefined in terms of the wavefield $U(\mathbf{x},\mathbf{x}_s)$. Because null-traces occupy locations $\mathbf{x}$ at which no data were collected, a multiple prediction can be also be written

$$M_{z=0}(\mathbf{x};\mathbf{x}_s,\omega) = \sum_{\mathbf{x}_a} U_{z=0}(\mathbf{x};\mathbf{x}_a,\omega)U_{z=0}(\mathbf{x}_a;\mathbf{x}_s,\omega)\,, \tag{5}$$

where the resultant volume has been regularized along $\mathbf{x}$ by adding zero-traces, and we have added the specification that the operation is being performed at the recording surface $z = 0$.

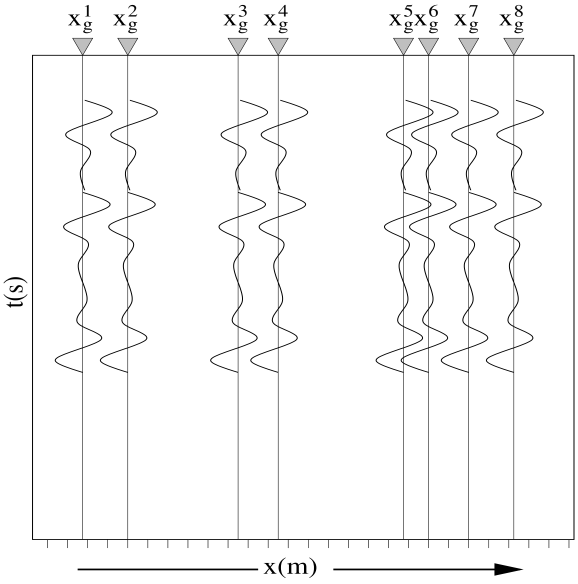

Figure 1: Traces from a shot-gather at locations $\mathbf{x}_g^i$ are inserted along the $\mathbf{x}$ axis to define the initial conditions for the upcoming wavefield U. brad1-GEO-2006-0199-fig1 [NR]

Using the principle of reciprocity between the receiver and source locations (first and second arguments of the wavefields respectively), the multiple prediction becomes

$$M_{z=0}(\mathbf{x};\mathbf{x}_s,\omega) = \sum_{\mathbf{x}_a} U_{z=0}(\mathbf{x};\mathbf{x}_a,\omega)U_{z=0}(\mathbf{x}_s;\mathbf{x}_a,\omega)\,, \tag{6}$$

where the subscript s on the RHS now represents simply a different receiver location (since it is the first argument of the wavefield), and the dummy index $\mathbf{x}_a$ is recognized as a summation over source location. Therefore, using arbitrary index subscripts c,d and restoring the significance of source location to subscript s

$$M_{z=0}(\mathbf{x}_c;\mathbf{x}_d,\omega) = \sum_{\mathbf{x}_s} U_{z=0}(\mathbf{x}_c;\mathbf{x}_s,\omega)U_{z=0}(\mathbf{x}_d;\mathbf{x}_s,\omega)\,. \tag{7}$$

Finally, we define the dummy indices c,d in terms of physically significant variables location and half-offset, $\mathbf{x}_c = \mathbf{x}+\mathbf{h}$ and $\mathbf{x}_d = \mathbf{x}-\mathbf{h}$, such that

$$M_{z=0}(\mathbf{x},\mathbf{h},\omega) = \sum_{\mathbf{x}_s} U_{z=0}(\mathbf{x}+\mathbf{h};\mathbf{x}_s,\omega)U_{z=0}(\mathbf{x}-\mathbf{h};\mathbf{x}_s,\omega)\,. \tag{8}$$

Thus reconfigured, equation 8 is now of parallel construction to the shot-profile imaging condition, equation 3, lacking only the summation over frequency.

Extrapolation by the exponential phase-shift operator $\exp(+i\omega k_z)$, in equation 1, simply redatums the shot-gather U. Image-space SRMP (IS-SRMP) is the application of a second imaging condition evaluated at each subsurface depth level during the migration that images only multiples. It is the chain of multiple prediction (convolution) and zero-time extraction (summation over frequency). The image-space multiple prediction, as a function of sub-surface offset, is therefore

$$m_z(\mathbf{x},\mathbf{h}) = \sum_{\mathbf{x}_s}\sum_{\omega} U_z(\mathbf{x}+\mathbf{h};\mathbf{x}_s,\omega)U_z(\mathbf{x}-\mathbf{h};\mathbf{x}_s,\omega)\,. \tag{9}$$

There are two important ramifications for the equation for predicting multiples with the imaging condition above. The first, is that this operation is intrinsically a shot-domain manipulation of the data. After sorting to CMP-offset coordinates, the source and receiver coordinates are mixed in such a way as to make IS-SRMP invalid for survey-sinking style migration algorithms. Second, because reciprocity was invoked to derive equation 9, off-end (marine) acquisition geometries will need to have split-spread gathers manufactured via reciprocity. The split-spread gathers will include the ray-paths from multiples that emerge in front of the receiver spread (boat) which need to be included in the shot-gathers to predict all possible multiple events.

Further understanding of the IS-SRMP imaging condition for those familiar with shot-profile migration algorithms can be elicited by defining the down-going wavefield in equations 1 & 2 by $D \equiv U$. Therefore, equations 1 - 3 become

$$U_{z+1}(\mathbf{k}_x;\mathbf{x}_s,\omega) = U_z(\mathbf{k}_x;\mathbf{x}_s,\omega)\exp(+i\omega k_z) \tag{10}$$

and

$$\hat{U}_{z+1}(\mathbf{k}_x;\mathbf{x}_s,\omega) = \hat{U}_z(\mathbf{k}_x;\mathbf{x}_s,\omega)\exp(-i\omega k_z) \tag{11}$$

with the imaging condition

$$m_z(\mathbf{x},\mathbf{h}) = \sum_{\mathbf{x}_s}\sum_{\omega} U_z(\mathbf{x}+\mathbf{h};\mathbf{x}_s,\omega)\hat{U}_z^*(\mathbf{x}-\mathbf{h};\mathbf{x}_s,\omega)\,, \tag{12}$$

where ˆ denotes that after extrapolation in different directions, the wavefields are no longer identical.

Because the conjugation of D in the imaging condition of equation 3 can be commuted with the causality of the extrapolation operator, it is not practically necessary to extrapolate U in two different directions. Instead, the second extrapolation step can be ignored

$$U_{z+1}(\mathbf{k}_x;\mathbf{x}_s,\omega) = U_z(\mathbf{k}_x;\mathbf{x}_s,\omega)\exp(+i\omega k_z) \tag{13}$$

and

$$U_{z+1}(\mathbf{k}_x;\mathbf{x}_s,\omega) = U_z(\mathbf{k}_x;\mathbf{x}_s,\omega)\exp(+i\omega k_z) \tag{14}$$

if the imaging condition is convolutional rather than correlational

$$m_z(\mathbf{x},\mathbf{h}) = \sum_{\mathbf{x}_s}\sum_{\omega} U_z(\mathbf{x}+\mathbf{h};\mathbf{x}_s,\omega)U_z(\mathbf{x}-\mathbf{h};\mathbf{x}_s,\omega)\,. \tag{15}$$

The migration defined by the chain of these extrapolation and imaging steps is exactly that for conventional migration where $D \equiv U$, instead of a modeled source function. Cast in this manner, the migration shows similarity with reverse-time migration (Baysal et al., 1983) and using multiples to migrate primaries (Shan and Guitton, 2004). The difference is in not time-reversing the data to use as the source function. IS-SRMP uses primaries as areal source functions and data to image multiples when energy is colocated in the wavefields after extrapolation.

Deconvolution

One of the reasons that multiple predictions must be adaptively subtracted from the data is that the wavelet in the data is squared during the convolution. To address the problem, we introduce deconvolution to both the conventional (Lee et al., 1991; Guitton et al., 2006) and the multiple prediction imaging conditions.

To normalize the frequency content and provide a sharper image, the imaging condition in equation 3 becomes

$$i_z(\mathbf{x},\mathbf{h}) = \sum_{\mathbf{x}_s}\sum_{\omega} \frac{U_z(\mathbf{x}+\mathbf{h};\mathbf{x}_s,\omega)D_z^*(\mathbf{x}-\mathbf{h};\mathbf{x}_s,\omega)}{\ll D_z(\mathbf{x}-h;\mathbf{x}_s,\omega)D_z^*(\mathbf{x}-h;\mathbf{x}_s,\omega)\gg}\,, \tag{16}$$

where the denominator is smoothed across horizontal coordinates for stability. In this implementation, the smoothing operator is a triangle function with a base five samples wide. Equation 9 can similarly be normalized/deconvolved and implemented

$$m_z(\mathbf{x},\mathbf{h}) = \sum_{\mathbf{x}_s}\sum_{\omega} \frac{U_z(\mathbf{x}+\mathbf{h};\mathbf{x}_s,\omega)U_z(\mathbf{x}-\mathbf{h};\mathbf{x}_s,\omega)}{\ll D_z(\mathbf{x}-\mathbf{h};\mathbf{x}_s,\omega)D_z^*(\mathbf{x}-\mathbf{h};\mathbf{x}_s,\omega)\gg}\,. \tag{17}$$

It could be argued that the deconvolutional imaging condition for multiples above should be normalized by a smoothed version of the power spectrum of U instead of D. However, in the interest of parallel construction, we have implemented it as above. If the wavelet used to model D accurately represents the amplitude and frequency content of the data, the choice of U or D as divisor will be of little importance. The benefit of a deconvolution imaging condition is to collapse the wavelet that events are convolved with as much as possible. Consequently, the image-space volumes $i_z(\mathbf{x},h)$ and $m_z(\mathbf{x},h)$ share approximately the same bandwidth and can be more easily subtracted from each other to provide an image space consisting of only primaries. If the data are not zero-phase before implementing IS-SRMP, deconvolution will not address phase-roll of the wavelet within the data introduced by squaring to compute the multiple prediction.

Analytic example

In 1D, let a trace be represented in the Fourier domain by the expression

$$R(\omega) = \mathrm{e}^{-i\phi_w} + \mathrm{e}^{-i\phi_e} - \mathrm{e}^{-i2\phi_w} - 2\mathrm{e}^{-i(\phi_w+\phi_e)} - \mathrm{e}^{-i2\phi_e} = P + M_1. \tag{18}$$

The trace has primary reflections, P, at phase delays, ϕ, representing a water-bottom and a subsurface event. Also included are first order multiples, M_1, which are the water-bottom multiple at $2\phi_w$, two peg-leg multiples at $\phi_w+\phi_e$, and the event multiple at $2\phi_e$. SRMP dictates the autoconvolution of P to derive M_1, which is clearly true. Including the events M_1 in the autoconvolution will derive the second order multiples as well.

Extrapolating trace R to a deeper depth applies a common phase shift, say $\mathrm{e}^{-i\phi_z}$, to all terms in equation 18. The trace then becomes

$$R_z(\omega) = e^{-i\phi_z}(\mathrm{e}^{-i\phi_w} + \mathrm{e}^{-i\phi_e} + \mathrm{e}^{-i2\phi_w} + 2\mathrm{e}^{-i(\phi_w+\phi_e)} + \mathrm{e}^{-i2\phi_e}) = e^{-i\phi_z}P + e^{-i\phi_z}M_1. \tag{19}$$

This equation shows that the extrapolation of data without multiple subtraction produces the superposition of the redatumed primaries and the redatumed multiples. The extraction of the zero-time lag in the imaging condition of migration states that energy in the wavefield should be mapped into the image domain only when the extrapolation phasor ϕ_z, is equal to the time delay of the event in the data. Thus the water bottom primary is imaged when $\phi_z = \phi_w$, the water-bottom multiple is imaged when $\phi_z = 2\phi_w$, etc. Whether the data R is first separated into its constituent parts, P and M_i, or not, it can be seen where in the image domain the various events in the above example will be placed.

However, by first squaring the trace, as dictated by the multiple prediction imaging condition (equation 9), the water-bottom primary is mapped into the image domain when $\phi_z = 2\phi_w$. This is the same phasor that maps the recorded water-bottom multiple into the image domain using the conventional imaging condition. Thus, the multiple prediction in the image space can be directly calculated with a multiple-only imaging condition due to the commutability of convolution and extrapolation.

For prestack data in higher dimensions, the phasor $e^{-i\phi_z}$ is the combination of the downgoing energy D and the exponential delay operators in equations 1 and 2.

SIGSBEE 2B SYNTHETIC EXAMPLES

The Sigsbee2B dataset was designed to model strong surface-related multiples from an offshore acquisition. Two datasets were generated with a 2D finite difference algorithm: One with the perfectly reflecting free surface, and one without[1]. Therefore, the direct subtraction of the two data volumes yields a perfect multiple model (modulo source and receiver ghost effects), without the need for SRMP. Though the data were modeled with an off-end acquisition strategy, split-spread gathers were computed via reciprocity for all of the examples below.

Figure 2 shows three versions of the bottom third of the image produced with the Sigsbee2b data sets. The top image used the data modeled without the reflecting free surface and contains only primaries. The middle image migrated the data with the free-surface and contains multiples as well. The bottom panel is the image produced by migrating the difference between the two data volumes (only multiples). The complex multiples in this deep section quickly overwhelm the primary events and could easily be mistaken for primaries in some instances. All panels, and the rest of the images herein, were produced with four reference velocities in a PSPI shot-profile migration code.

Figure 3a shows the zero subsurface-offset image from the data modeled without the free surface (multiple free). Panel b was produced with the same data and the IS-SRMP imaging condition, equation 8. By autoconvolving the upcoming wavefield U at every depth level in the image space, the right panel shows only multiples in the image domain using data containing only primaries. Note that there is no energy in Panel b above the first water-bottom multiple.

Figure 4 is directly analogous to the images in Figure 3, though employed the deconvolu-

[1] http://www.delphi.tudelft.nl/SMAART/S2Breadme.htm

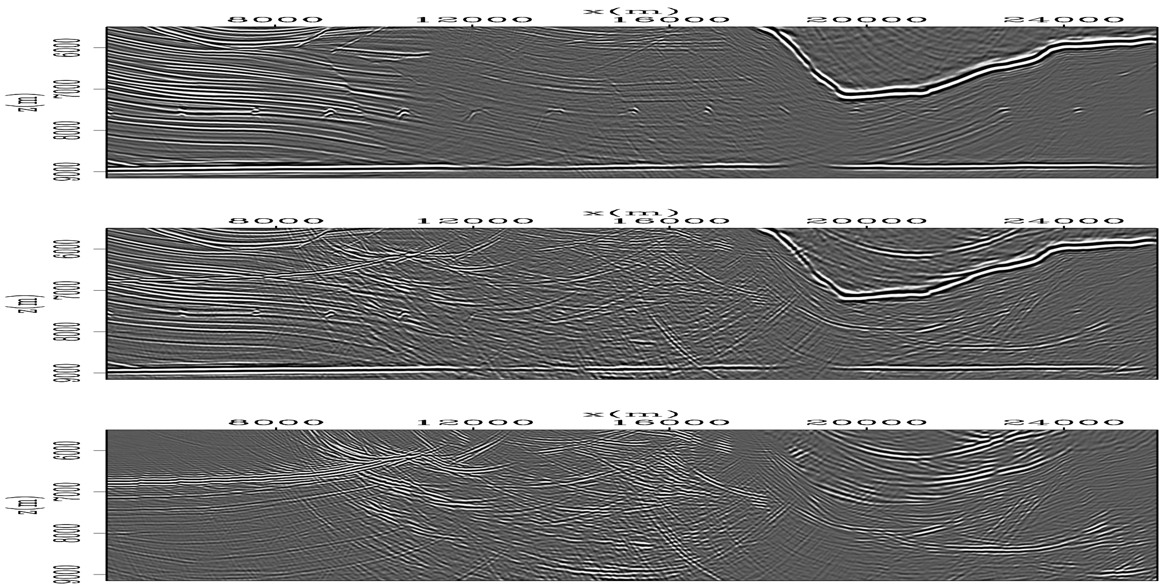

Figure 2: Images of the bottom third of Sigsbee2b modeled data. Top panel is migration of primaries only. Middle panel is migration of multiples and primaries. Bottom panel is migration of multiples only. brad1-GEO-2006-0199-fig2 [NR]

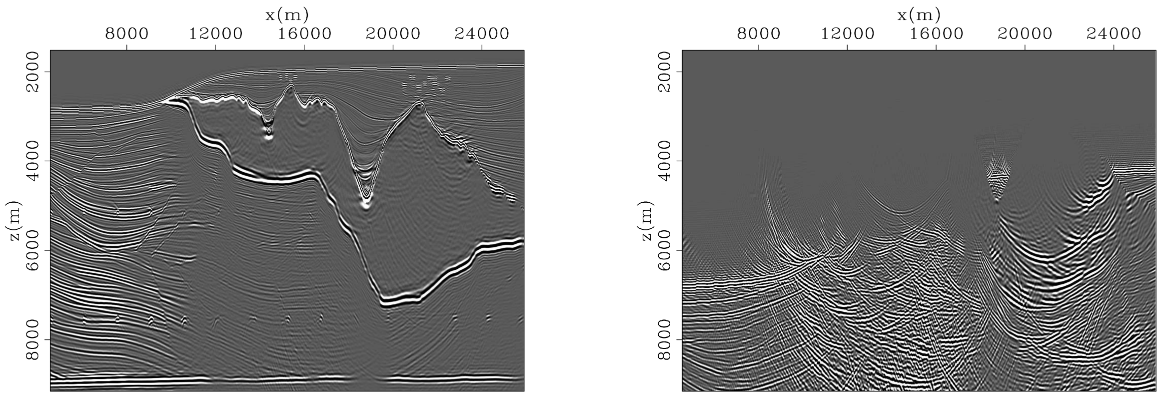

Figure 3: Zero subsurface-offset images of Sigsbee 2b data without the free surface. Panel `a` used conventional shot-profile imaging condition (equation 3). Panel `b` used the multiple prediction imaging condition for IS-SRMP. (equation 9). brad1-GEO-2006-0199-fig3 [NR]

tion imaging conditions from equations 16 & 17 respectively. Notice the increased bandwidth of the events in Panel b compared to the previous result and the increased quality of the steeply dipping salt bottom in Panel a. Also, in the shallow depths before the first water-bottom multiple and within the salt body, the multiple prediction shows increased noise/chatter. This can be muted before (adaptive) subtraction and should pose little problem.

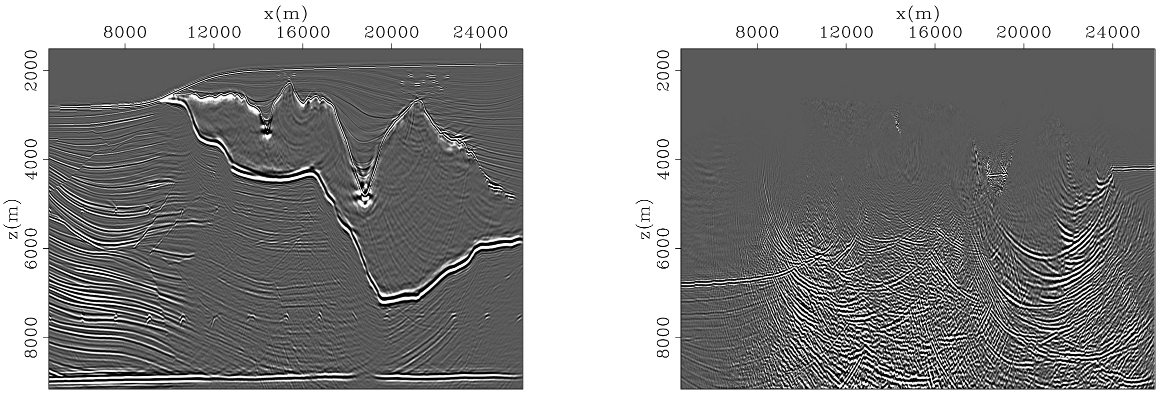

Figure 4: Deconvolutional imaging conditions used in contrast to Figure 3. Panel a used shot-profile imaging condition with deconvolution (equation 16). Panel b used the multiple prediction imaging condition with deconvolution (equation 17). brad1-GEO-2006-0199-fig4 [NR]

Figures 5 & 6 are images produced with conventional and deconvolutional imaging conditions, respectively, using the data containing primaries and multiples. The multiples below the salt body, which may be difficult to label as such without prior knowledge, are well predicted.

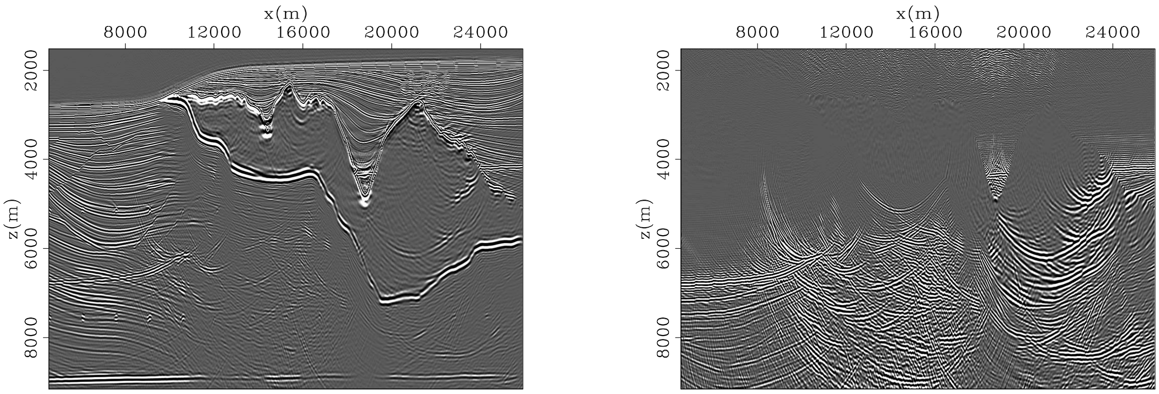

Figure 5: Zero subsurface-offset images of Sigsbee 2b data with the free surface. Panel a used conventional shot-profile imaging condition (equation 3). Panel b used the multiple prediction imaging condition (equation 9). brad1-GEO-2006-0199-fig5 [NR]

Guitton (2005) shows convincingly that pattern-based and adaptive subtraction of multiple models work much better when higher dimensinalities can be exploited by the subtraction algorithm. The various imaging conditions presented above can all calculate subsurface offset dimensions to facilitate better subtraction. Figure 7 shows the extension of the imaging conditions above to non-zero reflection angle (Sun et al., 2004). The data were migrated using

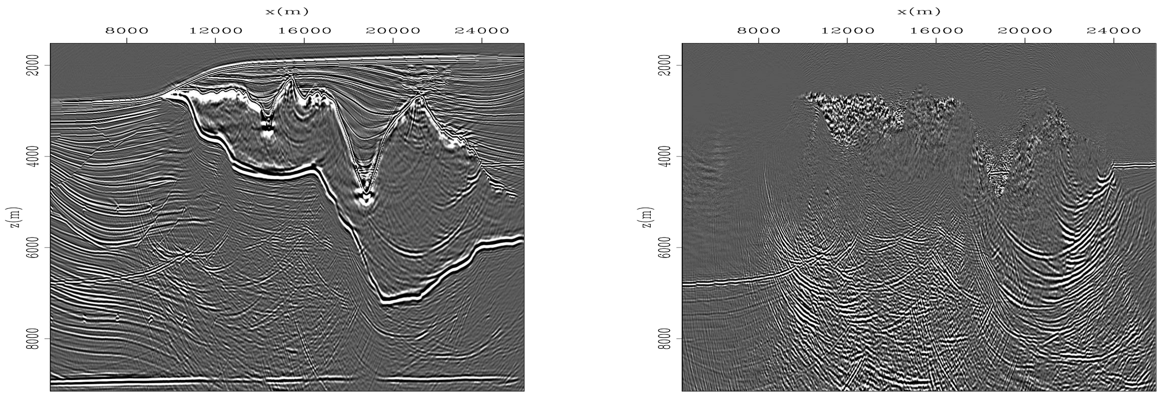

Figure 6: Deconvolutional imaging conditions used in contrast to Figure 5 (free surface included). Panel `a` used shot-profile imaging condition with deconvolution, (equation 16). Panel `b` used the multiple prediction imaging condition with deconvolution (equation 17). brad1-GEO-2006-0199-fig6 [NR]

the imaging conditions above, and then transformed to the angle domain after Sava and Fomel (2003). The data input to migration contained both primaries and multiples, and the imaging conditions used were not the deconvolutional variants.

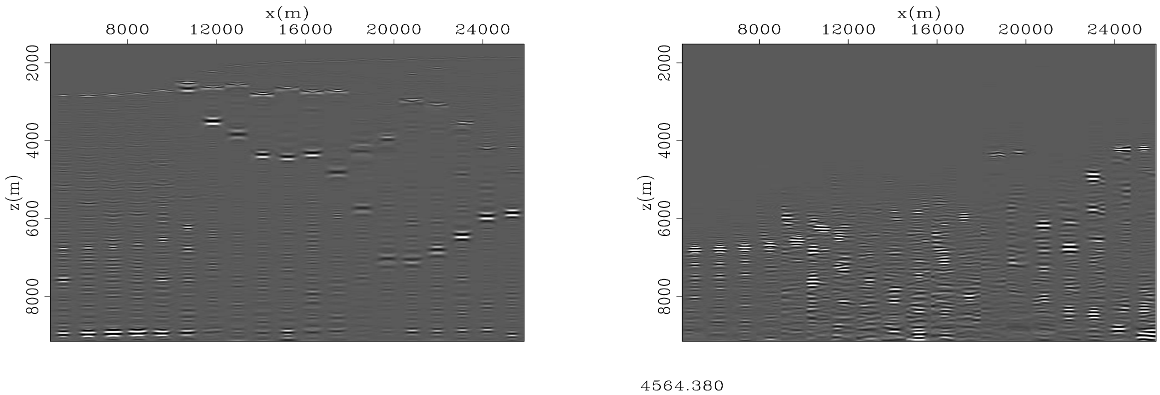

Figure 7: Angle-domain common-image gathers selected regularly across the image. Panel `a` used the conventional imaging condition (equation 3), Panel `b` the multiple prediction imaging condition (equation 9). The volumes were then transformed to incidence/reflection angle. brad1-GEO-2006-0199-fig7 [NR]

DISCUSSION AND CONCLUSIONS

Image space SRMP produces a multiple prediction by convolving the data with itself at every subsurface depth level during the course of a shot-profile migration. The result is the same as migrating the conventional SRMP multiple prediction. This method will only work with shot-profile migration strategies since the convolution operation must operate on distinct gathers rather than the combinations thereof produced by resorting to CMP coordinates. The simplicity of this approach can immediately be leveraged to manufacture the image-space multiple prediction directly from any shot-profile migration program. The method is immediately applicable to 3D, and non-zero subsurface-offset and angle. Any migration algorithm that maintains separate up-coming and down-going wavefields and uses a combinatory imaging condition (e.g. planewave and reverse-time migrations) can also be easily modified to produce an IS-SRMP volume.

Importantly, split-spread gathers must be pre-computed via reciprocity for data collected with off-end acquisition geometries. Off-end gathers will not contain (nor therefore predict) emerging rays which pierce the acquisition surface in front of the boat. This may increase the size of the computational domain used for propagating each individual shot-record. The cost increase by performing two imaging conditions is not severe, as the cost of calculating an imaging condition with in-line is usually a fraction of the cost of a shot-profile migration. Therefore, whenever a shot-profile migration is being performed, it may be advantageous to generate the IS-SRMP even if a data-space elimination effort has already been performed.

Given a reasonably accurate velocity model for migration, it is only necessary to compute $O(10)$ subsurface offsets. This results in many fewer traces involved in calculating the multiple prediction than the $O(1000)$ offsets collected at the surface. This savings will be offset however by the need to convolve the traces at every depth level, $O(100)$, of the image-space rather than just at the surface. Whatever the balance of floating-point operations for a particular survey, the convenience of being able to manufacture the multiple prediction during another required processing step will save file manipulation, sorting, and overhead costs. Further, this technique can also be used in a target oriented fashion by simply not calculating the multiple prediction where it is not needed, e.g. at shallow depths.

The quality of the multiple prediction produced in the image-space with this technique is independent of the accuracy of the velocity model used during the migration. The multiple prediction, propagated with the same velocity model, will be kinematically accurate with the location of any multiples in the migrated image. Though both the image and the multiple prediction may be incorrect due to the use of an inaccurate velocity model, it has to correspond with the image constructed with the same extrapolation operators and velocity model. Due to the squaring of the wavelet when convolving the data, the multiple prediction can not be directly subtracted from the data or the image. However, deconvolution imaging conditions or a-priori wavelet deconvolution can make great strides in this direction.

While IS-SRMP, by definition, produces only surface-related multiples, the technique could be manipulated to address strong multiple generators in the subsurface. A topic for further research, we believe a layer-stripping type approach could be used when the location of problematic multiple generators is well constrained. By redatuming to the top of a multiple generator, the technique described above can be started at this deeper depth with the modeled multiples now referencing the new datum surface rather than the acquisition surface.

REFERENCES

Alvarez, G., B. Biondi, and A. Guitton, 2004, Attenuation of diffracted multiples in angle domain common image gathers: 74th Ann. Internat. Mtg., Soc. of Expl. Geophys., Expanded Abstracts, 1301–1304.

Anstey, N. A. and P. Newman, 1966, The sectional auto-correlogram and the sectional retro-correlogram: Geophys. Prosp., **14**, no. 4, 389–426.

Baysal, E., D. D. Kosloff, and J. W. C. Sherwood, 1983, Reverse time migration: Geophysics, **48**, no. 11, 1514–1524.

Berkhout, A. J. and D. J. Verschuur, 1997, Estimation of multiple scattering by iterative inversion, part I: Theoretical considerations: Geophysics, **62**, no. 05, 1586–1595.

Biersteker, J., 2001, MAGIC: Shell's surface multiple attenuation technique: SEG, 71st Annual International Meeting, 1301–1304.

Claerbout, J. F., 1971, Toward a unified theory of reflector mapping: Geophysics, **36**, no. 03, 467–481.

Gazdag, J. and P. Sguazzero, 1984, Migration of seismic data by phase-shift plus interpolation: Geophysics, **49**, no. 02, 124–131.

Guitton, A., A. Valenciano, D. Bevc, and J. Claerbout, 2006, Robust illumination compensation for shot-profile migration: 68th Annual Conference and Exhibition, EAGE, Expanded Astracts, P265.

Guitton, A., 2005, Multiple attenuation in complex geology with a pattern-based approach: Geophysics, **70**, no. 4, V97–V107.

Lee, D., I. M. Mason, and G. M. Jackson, 1991, Split-step fourier shot-record migration with deconvolution imaging: Geophysics, **56**, no. 11, 1786–1793.

Rickett, J. E. and P. C. Sava, 2002, Offset and angle-domain common image-point gathers for shot-profile migration: Geophysics, **67**, no. 03, 883–889.

Sava, P. C. and S. Fomel, 2003, Angle-domain common-image gathers by wavefield continuation methods: Geophysics, **68**, no. 3, 1065–1074.

Sava, P. and A. Guitton, 2003, Multiple attenuation in the image space: 73rd Ann. Internat. Mtg., Soc. of Expl. Geophys., Expanded Abstracts, 1933–1936.

Sava, P. and A. Guitton, 2005, Multiple attenuation in the image space: Geophysics, **70**, V10–V20.

Shan, G. and A. Guitton, 2004, Migration of surface-related multiples: tests on the Sigsbee2B dataset: 74th Ann. Internat. Mtg., Soc. of Expl. Geophys., Expanded Abstracts, 1285–1288.

Sun, P., H. Liu, and S. Zhang, 2004, Imaging multiple reflections: The concept: 74st Annual International Meeting, SEG, Expanded Astracts, 1111–1114.

Tsai, C. J., 1985, Use of autoconvolution to suppress first-order long-period multiples: Geophysics, **50**, no. 09, 1410–1425.

Verschuur, D. J., A. J. Berkhout, and C. P. A. Wapenaar, 1992, Adaptive surface-related multiple elimination: Geophysics, **57**, no. 09, 1166–1177.

Weglein, A. B., 1999, Multiple attenuation: An overview of recent advances and the road ahead (1999): The Leading Edge, **18**, no. 1, 40–44.